PRECISION ASSESSMENT OF GRID IMPEDANCE ESTIMATION METHOD BASED ON PQ VARIATIONS APPLIED TO A THREE-PHASE PHOTOVOLTAIC CONVERTER UNDER VARIOUS GRID AND WEATHER CONDITIONS

Matheus Soares*, Marcello Neves*, Thiago Tricarico*, Felipe Dicler*, Gustavo Gontijo*, Mauricio Aredes*

*Laboratório de Eletrônica de Potência e Média Tensão - LEMT
Universidade Federal do Rio de Janeiro - UFRJ
Rio de Janeiro, RJ, Brasil

Emails: matheussoares@lemt.ufrj.br, marcello@lemt.ufrj.br, thiago@lemt.ufrj.br, dicler@lemt.ufrj.br, gustavo@lemt.ufrj.br, aredes@lemt.ufrj.br

Abstract— An electrical grid equivalent impedance, specially in the context of microgrids, may be time-varying due to disconnections. Therefore, online grid impedance monitoring is deemed important to detect islanding and to allow for adaptive control schemes. In this context, a series of methods for grid impedance estimation using active and reactive power orders variations has been proposed in the last decade. The objective of this work is to use simulations to analyze the precision of the three-phase, synchronous frame based version of this method when implemented in a grid-tie inverter for a photovoltaic system. Various combinations of short-circuit MVA and X/R ratios are tested. Estimation under multiple solar radiation conditions is also studied. Finally, the method is applied as an islanding detection algorithm and the compliance with the test setup required by IEEE 1547 is verified.

Keywords— Grid impedance estimation, Photovoltaic generation, Islanding detection.

1 Introduction

The ongoing growth of decentralized generation and the changing structure of the electric power system add new challenges to the organization of the grid. Under this new paradigm, specially taking into account the increase of power electronic converters associated to sources such as photovoltaic, evaluating the grid parameters constantly becomes important not only as an option to apply schemes such as adaptive control to the converter but as one of the possible ways of detecting islanding. Islanding is the situation where an isolated grid remains energized even without the utility power supply. It can be a problem for multiple reasons: it may pose a risk to line operators, the isolated portion of the grid may have voltage and frequency levels outside the standard, and the microgrid and the main grid can become desynchronized, generating undesirable electromagnetic transients at the moment of reconnection (Mahat et al., 2008), (IEEE Std Committee 21, 2011).

Multiple methods for estimating grid impedance in real-time has been developed in the last years, these methods are usually classified as either passive (non-invasive) or active (invasive). Passive methods are based on measurement of system parameters variation such as voltage and frequency, this kind of method relies on signals that are already present in the system. It has the advantage of not disturbing the network, but several drawbacks: the natural system disturbances may happen rarely, so estimations may happen very intermittently. Furthermore, the signal to noise ratio (SNR) may be prohibitively low for accurate estimations. Active methods, on the other hand, deliberately disturb the network and then acquire and process the resulting signals. These also have some drawbacks, namely: the network will be constantly disturbed by the estimation and better estimations will often require larger disturbances, another problem is the complicated post-processing required by some of these methods (Ghanem et al., 2017). In (Ciobotaru et al., 2007), an active estimation method that circumvents this computational-intensive post-processing requirement has been proposed .

The method uses variations of active and reactive power of the converter to bring the grid to two operation points and to subsequently estimate the impedance, as illustrated in Figure 1. That original paper presents the single-phase formulation for the method, a three-phase implementation based on Proportional-Resonant controllers was presented in (Timbus, Rodriguez, Teodorescu and Ciobotaru, 2007), (Je-Hee Cho et al., 2014) explores the Phase-Locked-Loop (PLL) dynamics effects on the method and proposes a simplified, decoupled version for three-phase implementation in the synchronous dq frame. (Timbus, Teodorescu and Rodriguez, 2007) implements a grid voltage control method loop to decrease grid voltage perturbations and avoid flickering.

To the best of the authors knowledge, no thoroughly analysis of the precision of this method (or its variants) under a large set of grid conditions has been performed, specially when applied to photovoltaic generation. Nor has an analysis of compliance to standards such as IEEE 1547 under an islanding detection regimen. This paper is an attempt to partially fill this gap and is

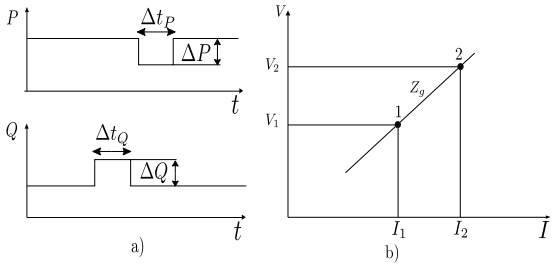

Figure 1: Impedance estimation using converter's power variations.

organized as follows: Section II presents the decoupled three-phase estimation method based on the synchronous frame, first presented in (Je-Hee Cho et al., 2014). Section III presents the control scheme necessary for the implementation of the method applied to a 12 kVA photovoltaic grid-tie inverter. Section IV shows the application of the method to a set of different grid and weather conditions and the resulting precision levels. Section V presents the application of the method to the anti-islanding test setup presented by IEEE 1547. Section VI contains the conclusions.

2 Instantaneous Three-Phase Power Based Active Impedance Estimation

The method presented in (Ciobotaru et al., 2007) is fundamentally based on the variation of active and reactive powers of the converter in order to cause a momentaneous operation in two different operation points. By doing so, it is possible to estimate the grid impedance Z_g (see Figure 2) by using the relations in (1).

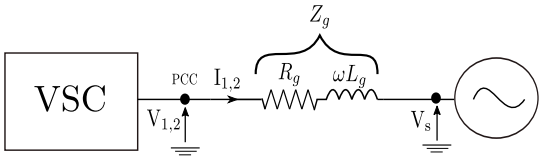

Figure 2: Converter connected to the grid.

$$\begin{aligned} V_1 = I_1 Z_g + V_s \quad V_2 = I_2 Z_g + V_s \\ V_1 - V_2 = Z_g (I_1 - I_2) \\ Z_g = \frac{V_1 - V_2}{I_1 - I_2} \end{aligned} \tag{1}$$

Considering that we are concerned with three-phase systems, the measured voltages and currents will be three-phase quantities. In this case, these quantities will be represented as complex vectors in a dq synchronous frame. By doing this, the final relation in (1) can be rewritten as (2) (Je-Hee Cho et al., 2014):

$$Z_g = \frac{(V_{1d} + jV_{1q}) - (V_{2d} + jV_{2q})}{(I_{1d} + jI_{1q}) - (I_{2d} + jI_{2q})} \tag{2}$$

Rewriting the right hand term in terms of variations (e.g $V_{1d} - V_{2d} = \Delta V_d$):

$$\frac{\Delta V_d + j\Delta V_q}{\Delta I_d + j\Delta I_q} = \frac{\Delta V_d + j\Delta V_q}{\Delta I_d + j\Delta I_q} \frac{\Delta I_d - j\Delta I_q}{\Delta I_d - j\Delta I_q} \tag{3}$$

Manipulating as shown in (3) and substituing back into (2) yields two terms, one real (equivalent to the grid resistance) and one complex (equivalent to the grid reactance):

$$\begin{aligned} R_g &= \frac{\Delta V_d \Delta I_d + \Delta V_q \Delta I_q}{\Delta I_d^2 + \Delta I_q^2} \\ \omega L_g &= \frac{\Delta V_q \Delta I_d - \Delta V_d \Delta I_q}{\Delta I_d^2 + \Delta I_q^2} \end{aligned} \tag{4}$$

An important observation has to be made, though: the voltage reference for the synchronous frame comes from a SRF-PLL (Synchronous Reference Frame Phase-Locked Loop, also known as dqPLL) using the voltage measurements at the point of common coupling (PCC). In this PLL, a PI controller is used to perform zero-tracking in the quadrature component of the positive sequence of the PCC voltage (Ali et al., 2018), the SRF-PLL diagram block is shown in Figure 3.

Considering a stationary frequency reference, the variations caused by the estimation method would be translated as two phenomena in the PCC voltage's complex vector: i) the variation of voltage in the direct axis would cause a scaling of the complex voltage vector; ii) the variation of voltage in the quadrature-axis would cause a variation in angle. However, the PLL doesn't yield a stationary frequency reference and nullifies the voltage in the quadrature axis. In other words, the PLL will track this angle variation and, disregarding the transient dynamics, nullify any ΔV_q (Je-Hee Cho et al., 2014).

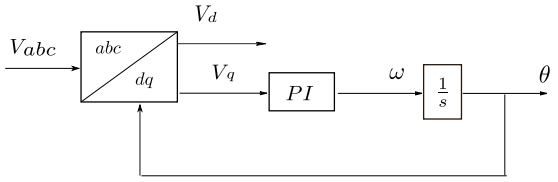

Figure 3: The Synchronous Reference Frame Phase Locked Loop (SRF-PLL) control diagram.

Even considering this simplified PLL effect, (4) shows that the estimation equations still present current coupling between the d and q axes, because variations of I_d and I_q still exist simultaneously.

By using relations presented in (Timbus et al., 2005), (Je-Hee Cho et al., 2014) proposes a simplified decoupled calculation. Equation (5) defines direct axis voltage variations in the PCC as function of current variations.

$$\Delta V_d = R_g \Delta I_d - \omega L_g \Delta I_q \tag{5}$$

By observing this relation, it becomes clear that, if the I_d and I_q orders of the converters are given in a decoupled manner, the estimation formulas for R_g and ωL_g are simply the ones shown in (6) and (7):

$$R_g = \frac{\Delta V_d}{\Delta I_d} \tag{6}$$

$$\omega L_g = \frac{-\Delta V_d}{\Delta I_q} \tag{7}$$

Writing the instantaneous active (p) and reactive (q) powers for the converter in the dq frame (Yazdani and Iravani, 2010):

$$\begin{aligned} p &= V_d\, I_d + V_q\, I_q \\ q &= -V_d\, I_q + V_q I_d \end{aligned} \tag{8}$$

Considering the PLL effects on the quadrature axis:

$$\begin{aligned} p &= V_d\, I_d \\ q &= -V_d\, I_q \end{aligned} \tag{9}$$

By using (9), it is possible to obtain current orders for power orders based estimation with a simplified method.

$$\begin{aligned} I_d &= \frac{p}{V_d} \\ I_q &= \frac{-q}{V_d} \end{aligned} \tag{10}$$

An example of usual variations of the physical quantities are given in Figures 6, 7 and 8 for a estimation starting at the 1.8 s mark. It is important to observe that the voltages and currents presented are filtered, as required for a precise estimation (Timbus, Teodorescu and Rodriguez, 2007).

3 Application to a Three-Phase MPPT-based Photovoltaic System

Photovoltaic generation connected to the grid usually uses a Maximum Power-Point Tracking (MPPT) method to improve the efficiency of the incoming solar energy use (Shi et al., 2015). In this paper, the estimation method is applied to a PSCAD model of the 12 kVA VSC with LCL filter shown in Figure 4. This converter is connecting solar panels and their associated MPPT-controlled boost converter to the grid.

The control block diagram for the converter using the estimation method presented in Section II is depicted in Figure 5. During normal operation the current orders I_d and I_q come from, respectively, the dc-link voltage control and the order for reactive power. When the estimation must be performed, the current orders are given by the relations in Equation (10). The SRF-PLL structure is used as synchronizer, the PI controller shown in Figure 3 is tuned as done by (Ali et al., 2018): $K_p = 92$ and $T_i = 0.000235$.

Figure 4: The converter modeled in PSCAD for this work.

4 Precision Assessment for Different Conditions

None of the references cited so far make a comprehensive precision analysis with varying grid conditions attempting to replicate likely operation conditions of distributed generation, this is the objective of this Section.

4.1 Minimization of Disturbance Level

As far as the authors know, there is no analytical procedure to determine the minimum required power variation's amplitudes ΔP and ΔQ nor duration Δt for a estimation within a certain precision. With that, the power steps definition becomes empirical. (Timbus, Rodriguez, Teodorescu and Ciobotaru, 2007) presents several simulations with different levels for disturbances and obtains good precision (relative error smaller than 10%) for power disturbances smaller than 1% of the nominal values. In a subsequent paper, however, it became necessary to use high levels of disturbances (up to 20%) for a 3 kVA experimental setting (Timbus, Teodorescu and Rodriguez, 2007). Therefore, in this work it is understood that extreme minimization of amplitudes using only simulations could lead to results that would become useless for posterior experimental validation. Also taking into account that the converter's power used here is four times higher than the used by (Timbus, Teodorescu and Rodriguez, 2007), ΔP and ΔQ were set as 2.0% of the nominal apparent power.

The Δt used was reduced in relation to these references: while both use 0.5 s, in the present work the authors considered 0.3 s to be appropriate. The authors noticed that the choice of Δt and the tuning of the filter configure a trade-off: a filter with lower cut-off frequency will remove noise and result in better estimation, but the delay in the physical quantities of interest will make the use of longer disturbances necessary.

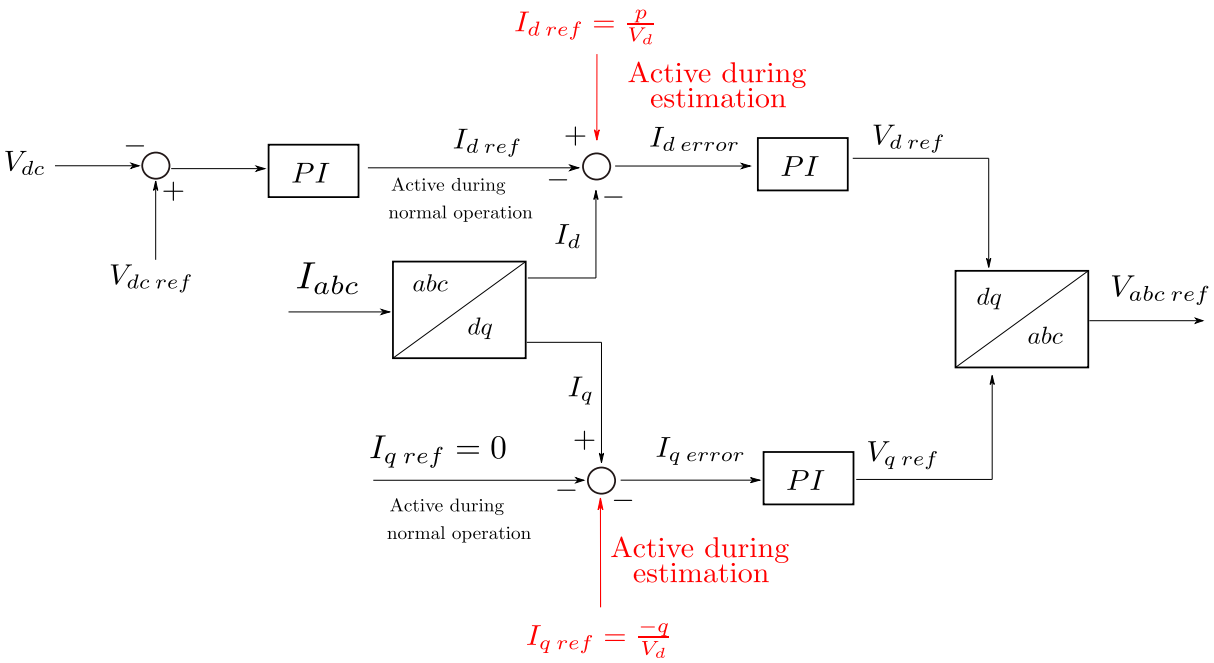

Figure 5: Converter current control with impedance estimation.

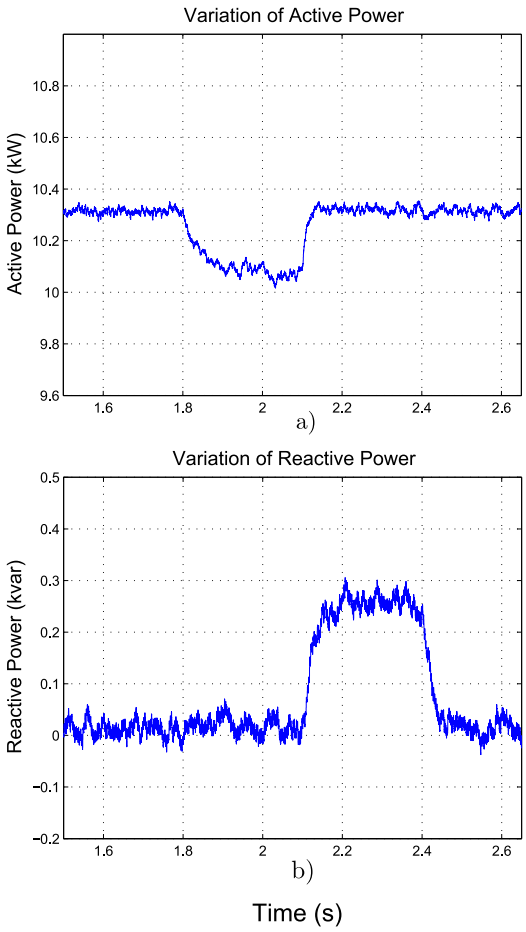

Figure 6: Variation of active and reactive powers during estimation: a) Active power; b) Reactive power.

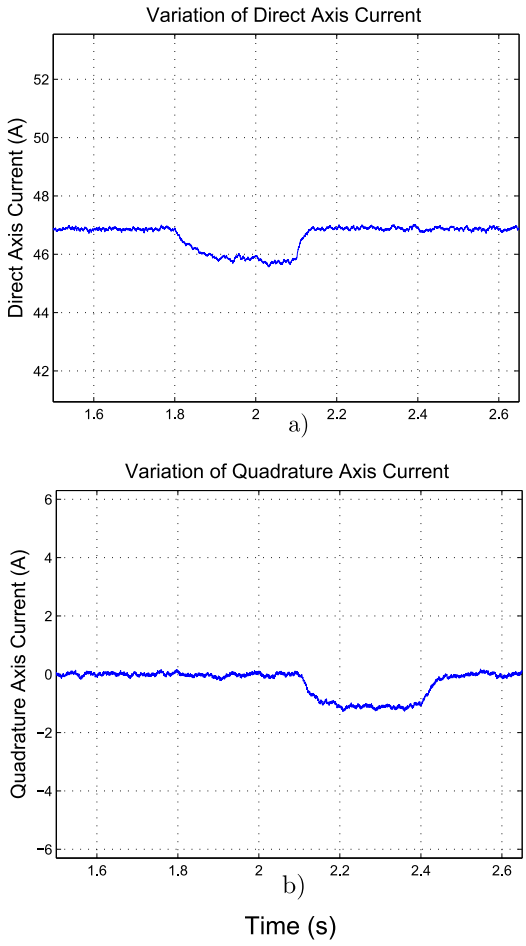

Figure 7: Variation of currents during estimation: a) Direct Axis Current; b) Quadrature Axis Current.

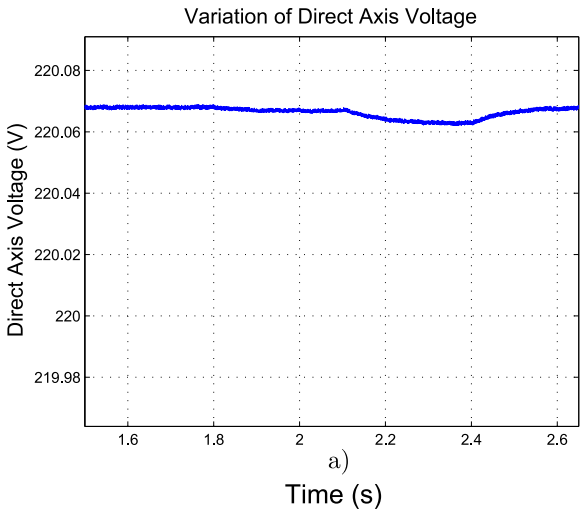

Figure 8: Variation of Direct Axis Voltage during estimation.

4.2 Precision under Various Grid Conditions

Using the step quantities presented in Subsection 4.1, a set of simulations has been performed in order to obtain relative errors for Impedance (Z), Resistance (R) and Inductance (X). These quantities are used to assess the precision of the method under different grid conditions. The short-circuit MVA level has been varied within an approximate 30 MVA range and, for each of these levels, the X/R ratio was varied between 3 and 30. These values attempt to encompass conditions compatible with isolated systems and grid-connected systems in relatively remote regions. Figures 9, 10 and 11 present the relative errors obtained from the studies.

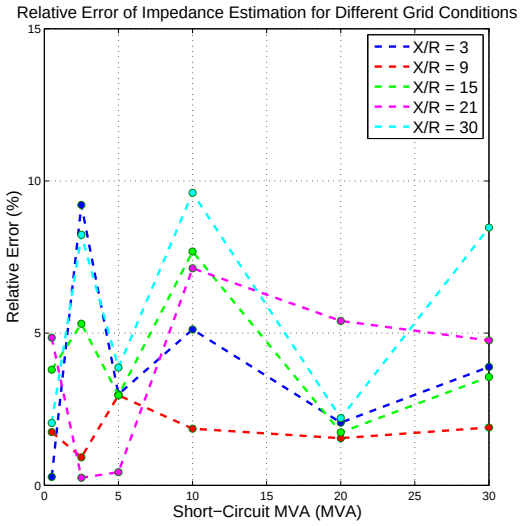

Figure 9: Relative error of impedance values for different grid conditions.

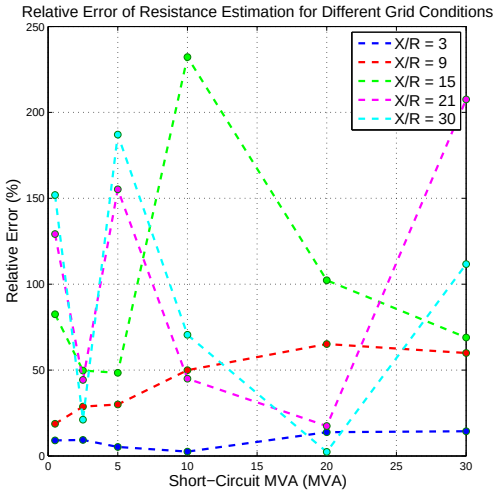

Figure 10: Relative error of resistance values for different grid conditions.

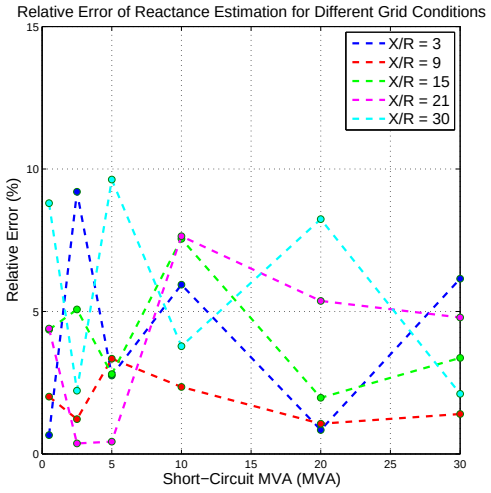

Figure 11: Relative error of reactance values for different grid conditions.

It can be seen that impedance and reactance estimation errors are relatively robust against grid conditions variations and, in every tested situation, remained within a 10% maximum limit. Precise resistance estimation, on the other hand, is severely affected by the X/R ratio. Amongst the studied cases, only the one using X/R ratio of 3 acquired estimation values within an upper relative error boundary of 15%. In every other studied circumstance, the resistance estimation relative error grew considerably and became unreliable. This fact, as can be seen in Figure 9, did not affect the impedance estimation precision. This is expected because, with growing X/R ratio, the influence of the reactance predominates in the total Z_g value.

4.3 Precision under Various Weather Conditions

The method is also applied under different fixed solar radiation (ϕ) conditions, and under two varying solar radiation conditions (to represent, for example, passing clouds). For a bus with short-circuit MVA of 10.0 MVA and X/R ratio of 5, five irradiation fixed-points are chosen, namely $1000\,\mathrm{W/m^2}, 825\,\mathrm{W/m^2}, 650\,\mathrm{W/m^2}, 425\,\mathrm{W/m^2}$ and $300\ \mathrm{W/m^2}$. The results for these tests are presented in Figures 12, 13 and 14.

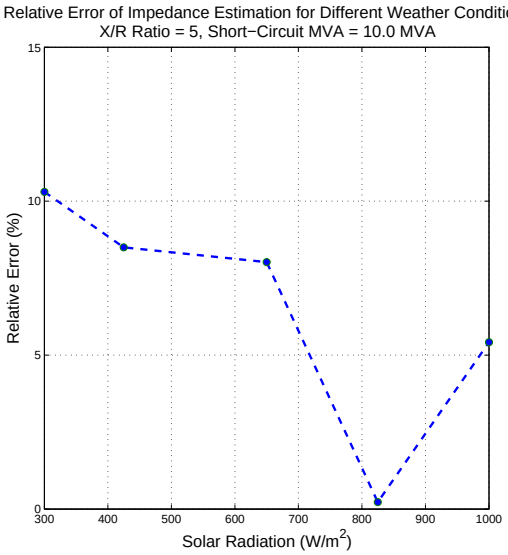

Figure 12: Relative error of impedance values for different weather conditions.

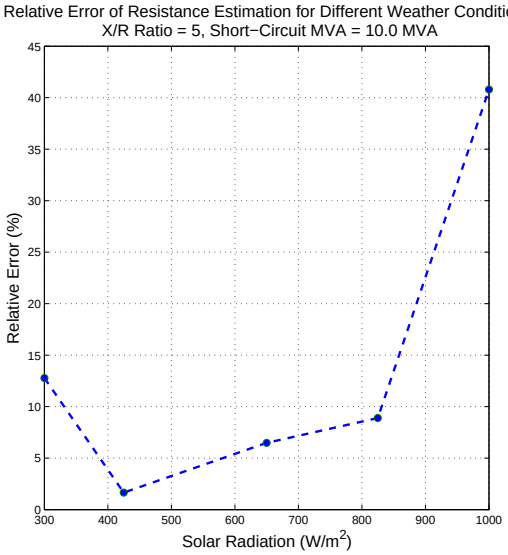

Figure 13: Relative error of resistance values for different weather conditions.

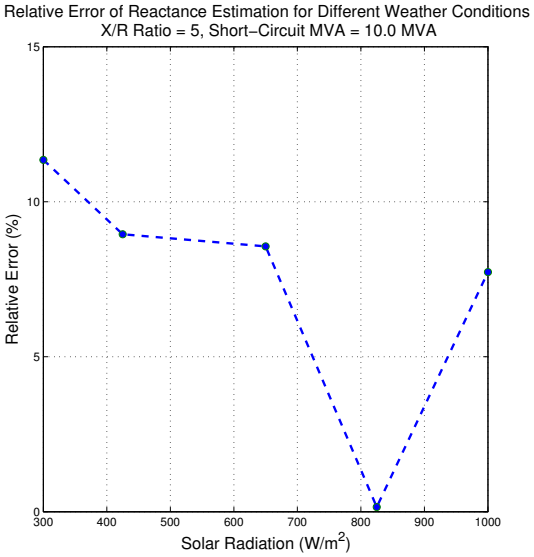

Figure 14: Relative error of reactance values for different weather conditions.

The estimation method is also tested under a $1000\ \mathrm{W/m^2}$ radiation with a superimposed time varying portion, as illustrated by Figure 15. The rates of variation applied were $\pm\ 7.5$ and $\pm\ 15\ \mathrm{W/m^2/s}$. The objective is to verify if a rapid change of solar radiation, caused for example by a fast moving cloud, brings difficulties to the estimation method. The values chosen were considered to be representative for this case of scenario, with base on the data of solar radiation variability presented by (Jayaraman and Maskell, 2012) and (Lave et al., 2015). The results are presented in Figure 16.

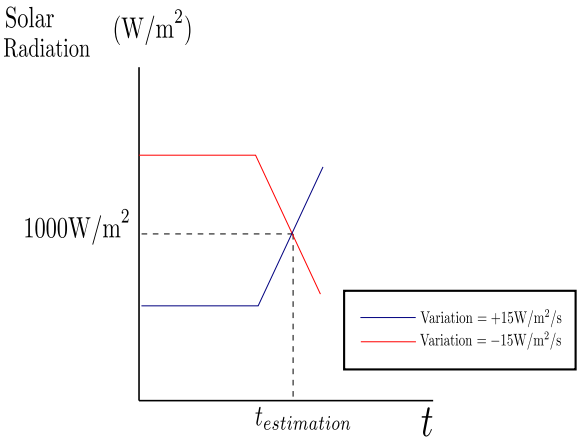

Figure 15: Two examples of estimation under varying solar radiation.

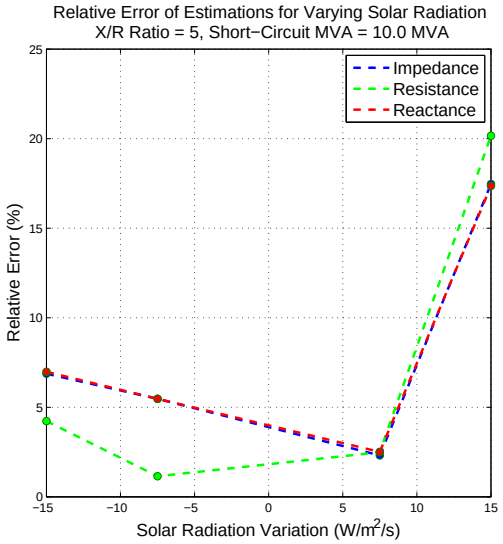

Figure 16: Relative error of estimations for varying solar radiation.

The trend observed in these results is that with sharper variations in solar radiation, poorer results of estimation are obtained. This is expected because power variations configure the basis of the method, variations from external sources will dampen or increase the originally intended power step and cause imprecisions. It also seems that the method is more sensible to positive variations of solar radiation, but there is no clear explanation for this phenomena at the moment.

5 Application as Islanding Detection

There are many international standards such as IEEE 1547, the european EN and the german VDE 0126 that estabilish minimum islanding detection and disconnection time for distributed generation. For a study of the feasibility of applying this method acting as an islanding detection method, simulations were performed following the IEEE 1547 test setup for anti-islanding techniques presented in (Teodorescu et al., 2011). This test setup consists, for three-phase systems, in the electrical connection of a balanced parallel RLC load as shown in Figure 17. According to the standard, the value of this RLC load must be adjusted until the current flowing to the utility becomes smaller than 2 % of the steady state value. Under this circumstance, switch S_1 is opened and the converter is disconnected from the grid. For an anti-islanding detection technique to be considered successful, this disconnection must be detected even under such conditions (Teodorescu et al., 2011).

In the case studied here, for a $1000\,\mathrm{W/m^2}$ solar radiation, the fundamental component of the steady state current has a $29.34\,\mathrm{A}_{rms}$ value. After the tuning of the RLC load, this value has decreased to $0.20\,\mathrm{A}_{rms}$, that is, to 0.68% of the original value. Virtually all the active power produced by the distributed generation is consumed by the RLC load. Within that configuration, the estimation method is then tested twice: before and after the electrical disconnection to the main grid. The relative error for impedance (Z_{error}) has been obtained in both situations and is presented in Table 1.

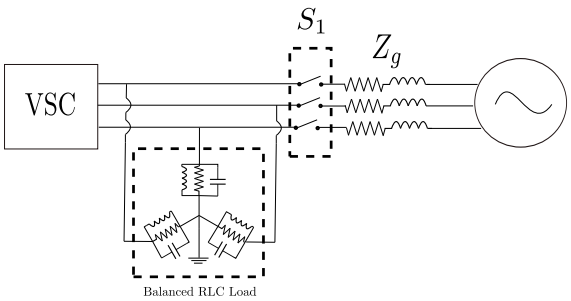

Figure 17: The anti-islanding test setup employed.

Table 1: IEEE 1547 Anti-islanding test setup results. Grid conditions: 10.0 MVA, X/R = 5

Condition	Z Error	Z Value
Normal	2.63 %	0.0048 Ω
Islanding	9.81 %	4.71 Ω

The method successfully estimated the impedance in both cases, with that, a specific sudden change in the impedance value detected by the method can act as a threshold for anti-islanding measures. It is important to notice that IEEE 1547 estabilishes that the distributed generation source must be disconnected within 2 seconds of the islanding event. Taking this into account, the estimation method must continuously inspect the grid condition with a time period smaller than the required 2 seconds.

6 Conclusions

The three-phase impedance estimation method based on decoupled power variations, proposed in (Je-Hee Cho et al., 2014), has been applied to a PSCAD/EMTDC model of a three-phase photovoltaic generation converter in order to make a initial study on the feasibility of using this method as a real-time impedance measurement procedure. Analyzing the simulations results it can be concluded that the method yields estimations for grid impedance with a relative error within the 10 % range, the authors believe that this error range is acceptable for most applications and specially for islanding detecting, where intense variations of impedance are expected (Teodorescu et al., 2011).

Another conclusion is that poor results for resistance estimations are expected with growing X/R ratio, this fact did not configure a problem

for the total impedance estimation, though. The relative simplicity of the method, added to the precision levels obtained in simulations, make it a good candidate for posterior experimental testing. An important observation is that multiple choices have to be made in order to implement the method. In experimental conditions, besides the choices of power-step amplitude and time duration, the precision of the measuring equipments has to be taken into account as well.

References

Ali, Z., Christofides, N., Hadjimetriou, L., Kyriakides, E., Yang, Y. and Blaabjerg, F. (2018). Three-phase phase-locked loop synchronization algorithms for grid connected renewable energy systems: A review, *Renewable and Sustainable Energy Reviews* **90**: 434–452.

Ciobotaru, M., Teodorescu, R., Rodriguez, P., Timbus, A. and Blaabjerg, F. (2007). Online grid impedance estimation for single phase grid-connected systems using PQ variations, *2007 IEEE Power Electronics Specialists Conference* pp. 2306–2312.

Ghanem, A., Rashed, M., Sumner, M., Elsayes, M. and Mansy, I. (2017). Grid impedance estimation for islanding detection and adaptive control of converters, *IET Power Electronics* pp. 1279–1288.

IEEE Std Committee 21 (2011). IEEE Guide for Design, Operation, and Integration of Distributed Resource Island Systems with Electric Power Systems.

Jayaraman, R. and Maskell, D. L. (2012). Temporal and Spatial Variations of the Solar Radiation Observed in Singapore, Vol. 25, pp. 108–117.

Je-Hee Cho, Ki-Young Choi, Yong-Wook Kim and Rae-Young Kim (2014). A Novel P-Q Variations Method using a Decoupled Injection of Reference Currents for a Precise Estimation of Grid Impedance, *IEEE Energy Conversion Congress and Exposition (ECCE)* , pp. 5059–5064.

Lave, M., Reno, M. and Broderick, R. (2015). Characterizing Local High-Frequency Solar Variability and the Impact to Distribution Studies, *Solar Energy* **118**: 327–337.

Mahat, P., Chen, Z. and Bak-Jensen, B. (2008). Review of Islanding Detection Methods for Distributed Generation, *2008 Third Conference on Electric Utility Deregulation and Restructuring and Power Technologies* pp. 2743–2748.

Shi, H., Zhuo, F., Yi, H., Wang, F., Zhang, D. and Geng, Z. (2015). A Novel Real-Time Voltage and Frequency Compensation Strategy for Photovoltaic-Based Microgrid, *IEEE Transactions on Industrial Electronics* **62**: 3545–3556.

Teodorescu, R., Liserre, M. and Rodriguez, P. (2011). *Grid Converters for Photovoltaic and Wind Power Systems*, Wiley-IEEE.

Timbus, A., Liserre, M., Teodorescu, R. and Blaabjerg, F. (2005). Synchronization methods for three phase distributed power generation systems - An overview and evaluation, *2005 IEEE 36th Power Electronics Specialists Conference* , pp. 2474–2481.

Timbus, A., Rodriguez, P., Teodorescu, R. and Ciobotaru, M. (2007). Line Impedance Estimation Using Active and Reactive Power Variations, *2007 IEEE Power Electronics Specialists Conference* , pp. 1273–1279.

Timbus, A., Teodorescu, R. and Rodriguez, P. (2007). Grid Impedance Identification Based on Active Power Variations and Grid Voltage Control, *2007 IEEE Industry Applications Annual Meeting*, pp. 949–954.

Yazdani, A. and Iravani, R. (2010). *Voltage-Sourved Converters in Power Systems: Modeling, Control and Applications*, Wiley-IEEE.